One-Step Preparation of pH-Responsive Polymeric Nanogels as Intelligent Drug Delivery Systems for Tumor Therapy

Yi Li, Quang Nam Bui, Le Thai Minh Duy, Hong Yu Yang, and Doo Sung Lee

Biomacromolecules, **Just Accepted Manuscript** • DOI: 10.1021/acs.biomac.8b00195 • Publication Date (Web): 06 Apr 2018

One-Step Preparation of pH-Responsive Polymeric Nanogels as Intelligent Drug Delivery Systems for Tumor Therapy

*Yi Li[1], Quang Nam Bui[1], Le Thai Minh Duy, Hong Yu Yang and Doo Sung Lee**

[1]*These authors contributed equally to this work*

School of Chemical Engineering and Theranostic Macromolecules Research Center, Sungkyunkwan University, Suwon, 16419, Republic of Korea

ABSTRACT: In this work, pH-responsive polypeptide-based nanogels are reported as potential drug delivery systems. By formation of pH-sensitive benzoic imine bonds, pH-responsive nanogels are constructed using hydrophilic methoxy poly(ethylene glycol)-b-poly[N-[N-(2-aminoethyl)-2-aminoethyl]-L-glutamate] (MPEG-b-PNLG) and hydrophobic terephthalaldehyde (TPA) as a crosslinker. At pH 7.4, MPEG-b-PNLG nanogels exhibit high stabilities with hydrophobic inner cores, which allow encapsulation of hydrophobic therapeutic agents. Under tumoral acidic environments (pH ~ 6.4), the cleavage of benzoic imine bonds induces the destruction of MPEG-b-PNLG nanogels and leads to rapid release of their payloads. The formation and pH-sensitivity of the nanogels are investigated by dynamic light scattering. These nanogels exhibit excellent stabilities in the presence of salt or against dilution. The globular morphologies of the nanogels are confirmed using transmission electron microscopy (TEM). Doxorubicin is used as a model drug to evaluate drug encapsulation and release. Finally, the anticancer activities of the drug-encapsulated nanogels are assessed *in vitro*.

KEYWORDS: Nanogels, pH-sensitive, Polypeptide, Drug delivery, Anticancer

INTRODUCTION

In the field of nanotherapy, nanogels have been considered as potential drug delivery platforms due to their outstanding advantages.[1] In general, nanogels are prepared by crosslinking of preformed polymeric nanoparticles or through template-assisted fabrication.[2] Nanogels, especially environment-responsive nanogels, are frequently employed as drug delivery systems (DDS), since they can fulfill many demands such as outstanding serum stabilities, high therapeutic efficiencies, low side effects and on-demand release of payloads. Intelligent nanogels that can respond to a wide range of stimuli (e.g. pH, temperature, redox, light and glucose) have been reported by many groups.[3, 4]

The high mortality rates caused by cancer have increased the need for drug delivery systems to improve the therapeutic efficiencies of anti-cancer drugs.[5, 6] To treat cancers more efficiently, smart drug delivery systems were widely developed based on the intrinsic features of various cancers (e.g. extracellular and intracellular acidities, hypoxia and disorganized vasculatures).[7, 8] Among these intrinsic features, acidic extracellular conditions, caused by anaerobic glycolysis in the hypoxic tumor microenvironment, is considered to be a major hallmark of tumor tissues.[9-11] Therefore, tumor extracellular pH-targeting drug delivery systems based on different mechanisms have been developed.[12-14] Similarly, pH-sensitive nanogels that are prepared using different polymers (both synthetic and natural),[15, 16] or different release mechanisms (pH-triggered swollen or disassembly)[17] also gained much attention for programmed drug delivery to deliver either hydrophobic or hydrophilic therapeutic agents.[18, 19] To date, pH-responsive nanogels are mainly prepared by two methods. One method is copolymerization of pH-responsive monomers and bifunctional crosslinkers. For example, Wang and coworkers copolymerized acrylic acid and N,N-bis(acryloyl)cystamine in the presence of 2,2-

azobis(isobutyronitrile) as an initiator.[18] The as-obtained nanogels can be further conjugated with poly(ethylene glycol) (PEG) and loaded with drugs to generate a core/shell-structured nanomedicine.[19] However, the nanogels prepared by this method is non-biodegradable and insensitive to subtle pH decrease (drug release is accelerated only when pH is decreased to 5). In addition, the preparation of drug-loaded nanogels is a complicated process and inconvenient for real application. The other method for pH-responsive nanogel preparation is crosslinking of pre-formed pH-responsive and self-assembled micelles. For example, Chen et al. synthesized a pH-responsive methoxyl poly(ethylene glycol)-b-poly-(N,N'-diethylaminoethyl methacrylate) copolymer and prepared a micelle solution from this diblock copolymer.[20] Next, a bifunctional crosslinker was employed to crosslink the cores of the micelles by quaternization reaction. When pH of the solution is decreased from 7.4 to 6.8, drugs can be released at a faster rate due to expansion of the nanogels at this pH. In another report, Yusa et al. fabricated a pH-responsive nanogel by photo-crosslinking of a pre-formed pH-responsive polymeric micelle.[21] However, these nanogels are non-biodegradable and cannot disassociate under acidic conditions.

In this study, we propose a new approach for fabrication of pH-responsive nanogels through a facile one-step method. A water-soluble polypeptide-based copolymer, methoxy poly(ethylene glycol)-b-poly[N-[N-(2-aminoethyl)-2-aminoethyl]-L-glutamate] (MPEG-b-PNLG), was directly crosslinked in an aqueous solution using terepthalaldehyde (TPA) at physiological pH (pH 7.4). The acid-labile benzoic imine bonds can be cleaved under mildly acidic condition (pH 6.4). The as-prepared nanogels can physically encapsulate therapeutic molecules with high stabilities under the protection of the MPEG shell. The mechanism of pH-triggered release of DOX from this nanogel system is briefly shown in **Scheme 1**. Under physiological pH, the cores of the nanogels can protect the payloads from nonspecific absorption and minimize side effects. Once

the drug-loaded nanogel system accumulates at tumor sites and is exposed to the tumor acidic conditions, the cores can be rapidly destructed due to the cleavage of benzoic imine bonds, resulting in enhanced accumulation of drugs at tumor sites. Compared with the other reported pH-responsive nanogels, our nanogels have advantages in three aspects; (1) preparation of nanogels as well as drug loading can be achieved in one step (direct crosslinking of solubilized polymer through dynamic linkers), which is convenient over the other reported methods; (2) the polymer we use is biodegradable and biocompatible, and the nanogels are responsive to subtle pH changes; (3) a decrease in pH leads to both the release of drugs and disassociation of the nanogels, which makes the clearance of the drug carrier possible after achieving their missions.

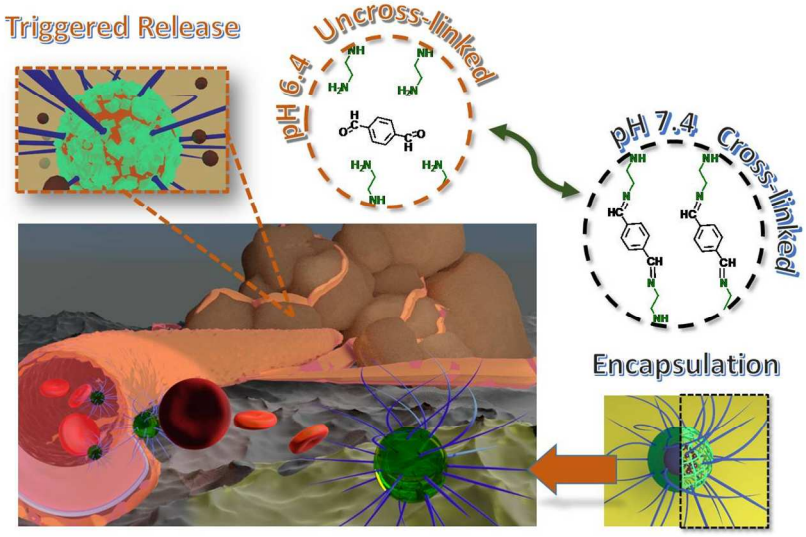

Scheme 1. Formation of pH-responsive MPEG-b-PNLG nanogels and their drug delivery mechanism.

EXPERIMENTAL SECTION

Materials. L-Glutamic acid γ-benzyl ester (BLG), 2-hydroxypyridine (2-HP), ethylenediamine (EDA), terephthalaldehyde (TPA), doxorubicin hydrochloride (DOX·HCl), triethylamine (TEA), chloroform ($CHCl_3$) and dimethylformamide (DMF) were purchased from Sigma-Aldrich (St. Louis, MO, USA). Triphosgene was obtained from Tokyo Chemical Industry Co., Ltd. Methoxy poly(ethylene glycol) amine (Mw = 5000 Da) was acquired from Sunbio.

Synthesis of γ-benzyl-L-glutamate-N-carboxyanhydride (BLG-NCA). Daly's method was used to prepare the BLG-NCA monomer.[22] Briefly, BLG (1 eq.) and triphosgene (0.6 eq.) were dissolved in anhydrous THF at 50°C for 1 hr. The reaction was terminated by pouring the mixture directly into cold hexane. The resultant solution was kept at -20°C overnight for recrystallization. The next day, the filtrate was further recrystallized twice in an ethyl acetate/hexane mixture with a volume ratio of 1:2 at -20°C for 12 hr.

Synthesis of methoxy poly(ethylene glycol)-block-poly(γ-benzyl-L-glutamate) (MPEG-b-PBLG). The precursor copolymer MPEG-b-PBLG was synthesized by ring-opening polymerization.[23-25] Briefly, MPEG-NH_2 (1 eq.) and BLG-NCA (40 eq.) were dissolved in 20 mL of anhydrous $CHCl_3$. The mixture was kept under nitrogen protection for 72 hr at room temperature (RT). The resultant polypeptide was collected by precipitation in cold ether and dried in vacuum oven at RT for 48 hr.

Synthesis of methoxy poly(ethylene glycol)-b-poly[N-[N-(2-aminoethyl)-2-aminoethyl]-L-glutamate] (MPEG-b-PNLG). MPEG-b-PNLG was synthesized by aminolysis of MPEG-b-PBLG using a large excess amount of ethylene diamine (EDA).[26] Briefly, a mixture of MPEG-b-PBLG and an excess amount of 2-HP was dissolved in anhydrous DMF at 55°C and kept under the protection of N_2. Subsequently, a large excess amount of EDA was added to the mixture, and

the mixture could stand for 72 hr. The yellowish and viscous product was collected by precipitation in cold ether. The crude product was purified by dialyzing the yellow liquid in a dialysis tube (3.5k MWCO) against HCl solution (0.01 M) for 1 day and deionized water (DIW) for another 2 days. The final MPEG-b-PNLG copolymer was obtained as a white powder after 3 days of lyophilization.

Characterization of polymers. The chemical structures of the copolymers (MPEG-b-PBLG and MPEG-b-PNLG), the nanogels and the nanogels after disassociation were analyzed using proton nuclear magnetic resonance spectroscopy (^{1}H-NMR). ^{1}H-NMR spectra were recorded on Varian Unity Inova 500NB (500 MHz) in dimethyl sulfoxide-d6 or D_2O at room temperature.

The molecular weights (Mn) of the polymers were measured by gel permeation chromatography (GPC) using DMSO as an eluent and a flow rate of 1.0 mL/min. The molecular weights were calibrated using PEG standards.

Preparation and characterization of nanogels. Firstly, 10 mg of MPEG-b-PNLG was dissolved in 10 mL of PBS or DIW at pH 7.4. Next, a solution of TPA (10 mg/mL in THF) was added to the above-mentioned aqueous copolymer solution, and the mixture was agitated for 1 hr at RT. After that, THF was removed using a rotary evaporator. The obtained solution was used for further characterizations.

FT-IR spectra of the MPEG-b-PNLG copolymer, nanogels and the nanogels after disassociation at low pH were recorded using an FT-IR spectrometer (IFS-66/S, Bruker, USA). The spectra were recorded in the range of 650 - 4000 cm^{-1} with a resolution of 4 cm^{-1}.

pH-responsibility of the nanogels. The surface charge and particle size of the nanogels (1 mg/mL) at various pH values were characterized by dynamic light scattering (Zetasizer, Nano-

ZS90). Different amounts of TPA were added to the MPEG-b-PNLG polymer solution to get different crosslinking densities (the molar ratio of CHO/NH_2 was adjusted from 0.2 to 1.2).

Stability and morphology of the nanogels. To check the stability of the nanogels against salt at 37^{o}C, the concentration of NaCl in the nanogel solutions was adjusted from 0 to 2 M. Moreover, to check the stability of the nanogels against dilution, the concentration of the nanogels in PBS was lowered gradually to 15.63 μg/mL. Then, the changes in particle diameter were measured and compared with one another. On the other hand, the stability of the nanogels during long term storage was also evaluated by size measurements. The morphologies of the MPEG-b-PNLG nanogels were observed using transmission electron microscopy (TEM) (JEOL USA, JEM-2100F). The TEM sample was prepared by a sequential two-droplet method with the tungstophosphoric acid solution (1% w/w in DIW) as a negative staining solution. Briefly, 10 μL of the nanogels in DIW (pH 7.4, 1 mg/mL, CHO/NH_2 = 1) was placed onto the dull side of the grid. The suspension was dried by tapping on a filter paper. Afterward, 20 μL of the staining solution was dropped onto the grid and removed after 30 seconds using filter paper. The stained grid was further washed twice with DIW to remove excess amounts of the staining agent and then allowed to be ambient-dried for a few hours before TEM scanning.

Drug loading and release. An anticancer drug, DOX·HCl (1 mg), was dissolved in 500 μL of THF that contains 5.2 mg of TEA for 24 hr. Then the DOX solution was filtered (via PTFE syringe filters, 0.22 μm) to remove the insoluble TEA·HCl salt. Subsequently, TPA (2.6 mg) was added to the above-mentioned solution. The DOX/TPA mixture was slowly dropped into MPEG-b-PNLG in PBS (7.4 mg in 10 mL) under vigorous stirring for 1 hr. THF was then evaporated under reduced pressure to get the DOX-loaded nanogel solution. The untrapped DOX, trace amount of THF and remaining TEA·HCl were further removed by dialysis (MWCO ~ 3.5K)

against 4 L of PBS at RT. The purified DOX-loaded nanogels were collected after lyophilization and then re-dispersed in PBS for UV-Vis measurements. Drug loading efficiency (DLE) and drug loading content (DLC) were calculated by the following equations:

$$\text{DLE (\%)} = \frac{\text{weight of loaded drug}}{\text{weight of feeding drug}} \times 100\%$$

$$\text{DLC (\%)} = \frac{\text{weight of loaded drug}}{\text{weight of nanogel}} \times 100\%$$

The release of DOX from the nanogels was measured by a dialysis method as published in our previous report with slight modifications.[27] A volume of 1 mL of the DOX-loaded nanogel solution (DOX concentration, 100 μg/mL) was dialyzed against 30 mL of PBS solution (pH 7.4 or 6.4) at 37^{o}C under a shaking speed of 100 rpm. A volume of 3 mL of exterior aqueous medium was collected at the following time intervals i.e., 1, 2, 4, 8, 12 and 24 hr, respectively. Afterward, an equal volume of fresh media was added. The concentrations of DOX in the collected samples were determined by UV-Vis spectroscopy with an absorption wavelength of 490 nm.

Cytotoxicity of MPEG-b-PNLG nanogels. Human embryonic kidney cell line 293T (supplied by ATCC, Manassas, VA, USA) was used to evaluate the biocompatibility of MPEG-b-PNLG nanogels through a MTT viability assay. The 293T cells were cultivated and seeded in 96-well plates at a concentration of 10^4 cells/well in Dulbecco's Modified Eagle's Medium (DMEM) (37^{o}C, 5% CO_2). After 24 hr, MPEG-b-PNLG nanogel solutions (in PBS) were fed to wells at various final concentrations (0 to 500 μg/mL). The 96-well plate exposed to different treatments was further incubated at 37^{o}C (5% CO_2) for another 24 hr. The plate was filled with 20 μL of MTT solution (5%) per well and subsequently incubated in the incubator for 2 hr (37^{o}C, 5%

CO_2). To dissolve the formazan crystals, DMSO was added to the plate (200 μL/well), which was darkly shielded and incubated at 60°C for 1 hr. A microplate reader was used to measure UV absorbance of MTT at a wavelength of 570 nm.

Cancer cell-killing effect of DOX-loaded nanogels. The human cancer cell line, MDA-MB-231 (ATCCHTB-26), was chosen as a model to evaluate the killing effect of DOX-loaded nanogels via a MTT assay (free DOX was used as the control group). A 96-well plate was prepared with 10^4 cells/well in Roswell Park Memorial Institute (RPMI) media. The cells were incubated with DOX-loaded nanogels or free DOX samples at various DOX concentrations (0, 5, 10, 15, 20, and 25 μg/mL) for 24 hr (37°C, 5% CO_2). The MTT assay was done to evaluate cell viability with a microplate reader (570 nm).

Cell uptake. MDA-MB-231 cells were seeded onto the 35-mm cell culture dish (10^6 cells/dish). DOX-loaded nanogels and free DOX samples were treated with the cells at the final DOX concentration of 3 μg/mL. The internalization was characterized via fluorescence-activated cell sorting (FACS), with PBS as a negative control. By varying treatment times (1 and 3 hr), the live cells were trypsinized and collected through washing cycles via centrifugation, which was then dispersed again in 200 μL of PBS. The fluorescence absorbance of cells that had taken up the drug was monitored via a flow cytometry instrument (MACSQuant Analyzer 10, Miltenyi Biotec.) using a population of 20,000 cells.

The cellular uptake of DOX-loaded nanogels and free DOX were further confirmed using confocal laser scanning microscopy (CLSM, LSM700 Carl Zeiss) X400. Briefly, MDA-MB-231 cells were prepared in confocal disks ($1x10^4$ cells) in RPMI. The cells were incubated with different DOX formulations at a final concentration of 3 μg of DOX per mL for different

treatment periods (1 and 3 hr). Nuclei were stained with 4, 6-diamidino-2-phenylindole (DAPI) for 10 min and washed twice with PBS before being fixed with 3.7% formaldehyde. Afterward, the cells were observed using CLSM.

RESULTS AND DISCUSSION

The route for synthesis of the copolymer MPEG-b-PNLG is illustrated in **Scheme 2**. The chemical structures of both MPEG-b-PBLG and MPEG-b-PNLG were determined by ^{1}H-NMR. The number of repeating units of the PBLG block was calculated using the ratio between the integrations of the peak corresponding to the methyl groups of MPEG (a, CH_3-, 3.14 ppm) and that of the methylene groups (f, -CH_2-, 5.17 ppm) (**Figure 1C**). The disappearance of benzyl groups together with the appearance of the ethyl groups of EDA (peak i and peak j in **Figure 1B**) confirmed the complete aminolysis of the benzyl groups. These results were summarized in **Table 1**. Ring-opening polymerization is a living polymerization that allows the molecular weight of the obtained polymers to be similar with the designed molecular weight. A series of polypeptides with structures similar to PNLG have been investigated using different diamine compounds for various applications in previous publications.[23-26] Since MPEG-b-PNLG is fully soluble in D_2O, all NMR peaks can be identified in the NMR spectra. However, after crosslinking the PNLG blocks using TPA in D_2O with NaOD as a pH-adjusting agent, the formation of benzoic imine bonds led to the formation of a hydrophobic PNLG/TPA core which was protected by MPEG shells. Therefore, only proton peaks corresponding to the MPEG block appeared in the NMR spectra. In **Figure 1A**, the disappearance of pendant amino groups in the spectra confirmed formation of nanoparticles with MPEG blocks as hydrophilic shells. This phenomenon has also been observed in several studies that are related to amphiphilic polymeric nanoparticles.[28, 29] Figure 1D shows the NMR spectrum of the MPEG-b-PNLG nanogels after

disassociation at pH 6.4. It can be seen that the peaks that belong to the PNLG block appeared again in the spectrum, which revealed the disassociation of MPEG-b-PNLG nanogels at low pH. Moreover, peak k in Figure 1D corresponds to the protons on the benzene rings of the TPA crosslinker. The molecular weight (Mn) and molecular weight distribution of MPEG-b-PNLG copolymer were measured by GPC. A unimodal peak is observed in Figure S1, and the copolymer has a Mn of 10,776 Da and a polydispersity index of 1.18.

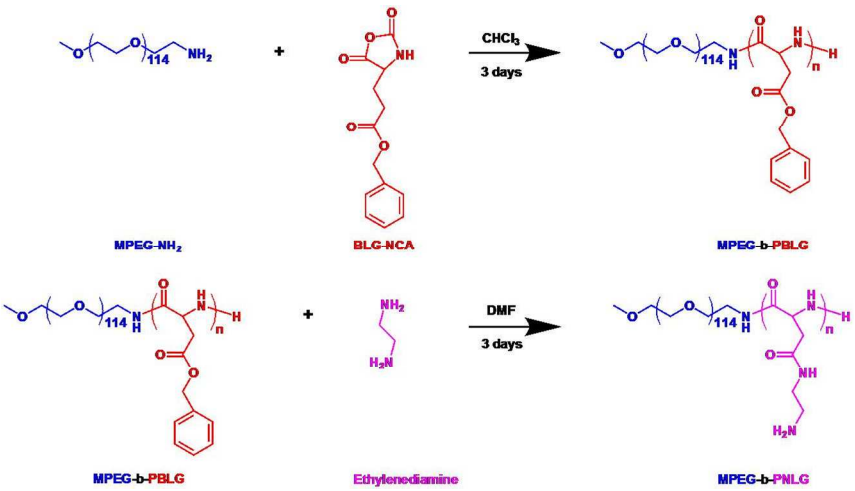

Scheme 2. Synthesis routes of MPEG-b-PBLG copolymer and MPEG-b-PNLG copolymer.

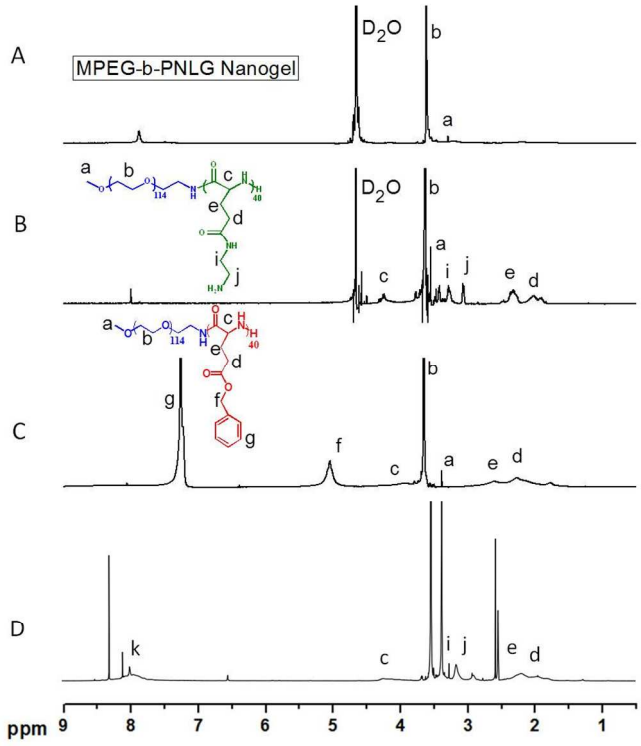

Figure 1. [1]H-NMR spectrums of (A) MPEG-b-PNLG nanogels, (B) MPEG-b-PNLG copolymer, (C) MPEG-b-PBLG copolymer, and (D) MPEG-b-PNLG nanogels after disassociation.

Table 1. Characterizations of copolymers and nanogels.

Sample	Molecular Weight[a)] (g/mol)	Particle Size[b)] (nm)	DLE[c)] (%)	DLC[c)] (%)
MPEG-b-PBLG	13,769	-	-	-
MPEG-b-PNLG	11,848	-	-	-
Blank nanogels	-	56.83	-	-
DOX-loaded nanogels	-	109.1	64.6	6.07

[a)] Calculated from ^{1}H-NMR spectrums; [b)] Determined from DLS; [c)] Calculated from UV-Vis absorbance.

The dynamic light scattering method was used to confirm the formation of the nanogels and to study the reversibility of the crosslinking. At pH 7.4, benzoic imine bonds between the primary amines pendant groups of PNLG blocks and benzaldehyde groups of TPA were formed, which subsequently induced nanoscale gelation and resulted in nanoparticles with a mean size of 56.83 ± 1.99 nm. In order to investigate the reproducibility of the sizes of nanogels, statistics on sizes of MPEG-b-PNLG nanogels from different batches is provided (Table S1). Dynamic light scattering also confirmed that the pH-induced formation of the nanogel is reversible; when the pH is decreased from 7.4 to 6.4, the nanogels disassociated and the polymer chains were dissolved in water. The size change in this process was shown in **Figure 2A**. The nanogels have a mean size of 56.83 nm at pH 7.4; while, at pH 6.4, no particles were detected. When pH was increased from 6.4 to 7.4, the nanoparticles with a similar mean particle size (53.26 ± 1.66 nm) can be formed. As expected, the surface charges of the nanogels (**Figure 3A**) showed similar zigzag tendencies when the pH was adjusted between 7.4 and 6.4 (the changes of zeta potential values between pH 6.4 (18.9 and 20.1) and pH 7.4 (7.21 and 9.15) are also reversible). Figure S2A shows the count rate of the MPEG-b-PNLG nanogel solution at different time after the addition of TPA into the MPEG-b-PNLG polymer solution. It can be seen that the number of nanogel particles gradually increases within 40 min after the addition of TPA but does not further increase after 40 min, which means the balance time for formation of nanogel particles is around 40 min. Digital images in **Figure 2D** show MPEG-b-PNLG solutions in PBS at pH 7.4 and pH 6.4. At pH 7.4, the solution possessed a higher turbidity due to the formation of nanoparticles; while, at pH 6.4, the solution was highly transparent due to the cleavage of the

imine bonds. Furthermore, by controlling the crosslinking density via controlling the ratio of CHO/NH_2, the number of particles was observed to increase remarkably when the ratio increased from 0.2 to 1.2 (**Figure 2B**). The increase of the count rate indicated that a higher amount of crosslinker led to the formation of more benzoic-imine bonds and thus produced more nanogel particles. Similarly, an increase in particle size was also observed when the CHO/NH_2 ratio was increased from 0.2 to 1.2 (Figure S2B), which provided a way to control the size of nanogels. The formation of nanogels at pH 7.4 and the disassociation of nanogels at pH 6.4 were further confirmed by FT-IR analysis. It can be seen from Figure S3 that a strong absorbance peak (1650 cm^{-1}) that corresponds to the bending vibration of N-H bonds in the primary amines of MPEG-b-PNLG is clearly observed. After the formation of nanogels, the disappearance of this peak demonstrated the disappearance of primary amine groups; while the appearance of the absorbance peak at 1590 cm^{-1} that corresponds to the stretching vibration of C=N bonds clearly proved the formation of imine bonds in the nanogels. When the nanogels are disassociated at low pH, the absorbance peak at 1590 cm^{-1} shifted to 1650 cm^{-1} again, demonstrating the cleavage of imine bonds and formation of primary amine bonds.

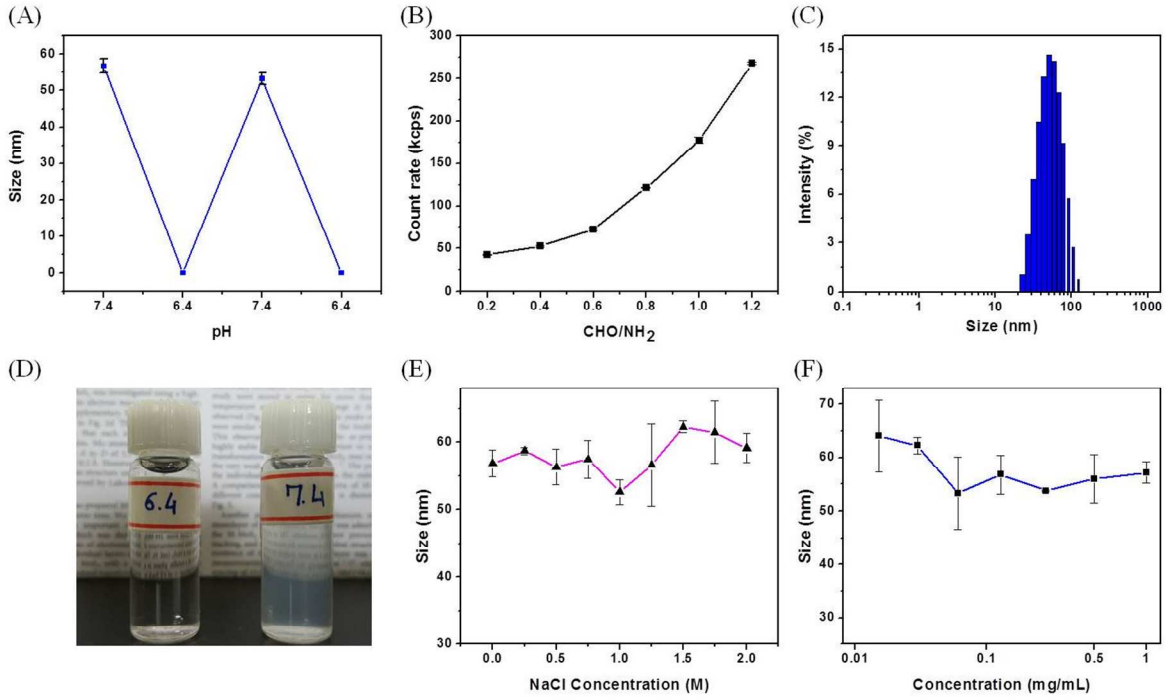

Figure 2. (A) Reversible size changes of MPEG-b-PNLG nanogels between pH 7.4 and 6.4. (B) Count rates of MPEG-b-PNLG nanogel solutions with various CHO/NH_2 ratios. (C) Size distribution of MPEG-b-PNLG nanogels. (D) Digital image of nanogel solutions at pH 6.4 and 7.4. Stability of MPEG-b-PNLG nanogels at various conditions (E) addition of NaCl, and (F) dilution of nanogel solution.

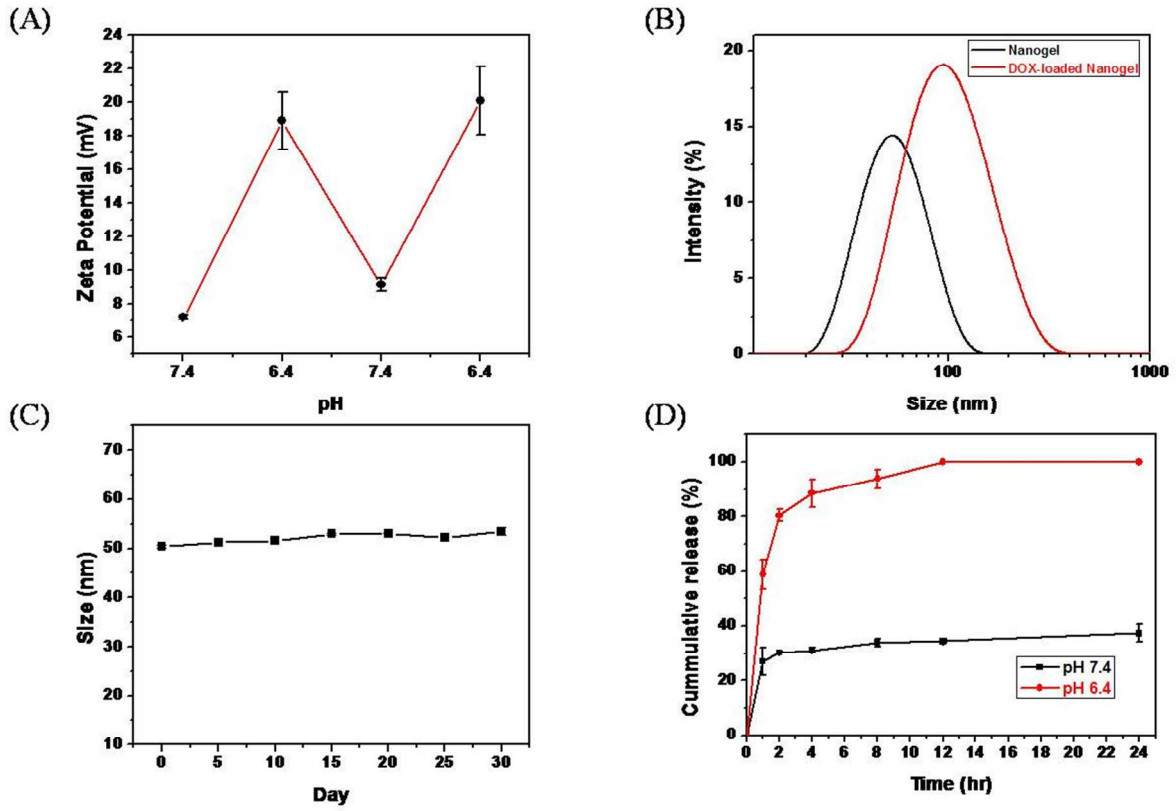

Figure 3. (A) Reversible zeta potential changes of MPEG-b-PNLG nanogels between pH 7.4 and 6.4. (B) Size distribution comparison of blank nanogels and DOX-loaded nanogels. (C) Stability of MPEG-b-PNLG nanogels with different incubation periods at 37°C. (D) Drug release profiles of DOX-loaded nanogels at different pH values.

To study the stabilities of the nanogels, the size change of the nanogels against incubation time, addition of salt and dilution were evaluated. **Figure 2E** showed that there were negligible changes in the size of the nanogels when the salt concentration increased from 0.25 M to 2 M, and **Figure 2F** showed the nanogels were stable when the concentration of the nanogel solutions was diluted from 1 to 0.01 mg/mL. In human blood, sodium salts are the main osmoles that keep various essential functions such as regulating blood volume, hydrostatic pressure, and osmotic equilibrium.[30, 31] Sodium chloride, a strong electrolyte, may critically influence the behavior of

the polymer molecules and lead to destabilization of drug delivery systems.[32] The existence of the TPA core may prevent PNLG blocks from conformational changes under the investigated conditions, which endows the crosslinked system with high stability. **Figure 3C** showed that the nanogels remained stable after 30 days of incubation at 37^{o}C. All these results suggest that the MPEG-b-PNLG nanogels are suitable for drug delivery applications where high stability and long term circulation is required.

A model drug, DOX, was encapsulated into the nanogels with a loading efficiency of 64.6% and a loading content of 6.07% by a solvent evaporation method. The size difference between the empty nanogels and the DOX-loaded nanogels were given in **Figure 3B**; The DOX-loaded nanogels have an average size of 109.1 nm that was higher than the size of the empty MPEG-b-PNLG nanogels. This observation confirmed the successful encapsulation of DOX. This volume increase might be caused by a higher hydrophilicity of PNLG blocks that limited DOX-loaded particles from forming a dense core.[33] The morphologies of MPEG-b-PNLG nanogels and DOX-loaded nanogels were observed by TEM. It can be seen from Figure S4 that there is not much morphological difference before and after loading of DOX. Since the TEM images are taken in dried states, the size difference of MPEG-b-PNLG nanogels and DOX-loaded nanogels is also not much. DOX-loaded nanogels were dialyzed in pH 7.4 or 6.4 media that simulate the physiological or tumoral pH, respectively. The segregated DOX concentration in the exterior media was measured and calculated to obtain the pH-dependent drug release profile (**Figure 3D**). At a physiological pH, the drug-loaded nanoparticles with highly stable benzoic imine bonds prevented leakage of DOX. Only 26.92% and 37.3% of DOX were released after 1 and 24 hr, respectively. In contrast, due to the cleavage of the acid-labile bonds in the core of the nanogels, the release rate was significantly accelerated with 58.81% and 100% of drug released after 1 and

24 hr, respectively. It is worth noting that a burst release of DOX from the nanogels is observed within the first hour even at pH 7.4. This might be attributed to the rapid release of unremoved free DOX or DOX that is adsorbed on the surface of the hydrophobic core of the nanogels.

The biocompatibilities of MPEG-b-PNLG nanogels were assessed by the MTT assay using 293T cell lines. **Figure 4A** showed that the nanogels exhibited negligible toxicities against the cells at both pH 7.4 and pH 6.4. The viability of the MDA-MB-231 human carcinoma cancer cell line was evaluated at different concentrations of DOX by a MTT assay to confirm the cancer cell-killing effect of the DOX-loaded nanogels. **Figure 4B** showed that the DOX-loaded nanogels exhibited higher cytotoxicity than free DOX against the breast cancer cell line MDA-MB-231. When incubating the cells with DOX-loaded nanogels, the cell viability decreased to 35.13 % and 18.29%, respectively, at a DOX concentration of 10 and 35 μg/mL (IC50=3.66 μg/mL). In contrast, 57.93% and 32.11% of the cells survived after treatment with free DOX at a concentration of 10 and 35 μg/mL, respectively (IC50=15.45 μg/mL). The MDA-MB-231 cell line has been reported to be relatively resistant to DOX, which may be acquired during treatment via various mechanisms such as mutation of the tumor suppressor protein p53, MDR1 over-expression, or drug efflux.[34] This acquired resistance reduces the activity of DOX on killing cancer cells; so, normally a higher dose of DOX with longer treatment time is needed.[35, 36] To overcome these resistances, various promising carriers that preserve the activity of DOX but avoid its side effects have been studied. By conjugating DOX with cell-penetrating peptides (e.g., TAT, Penetratin, and Maurocalcine), several reported systems could induce cell apoptosis with higher cell-killing efficiency than free DOX.[37, 38] Polymer-based vectors have also been developed to enhance tumor accumulation as well as to reach an outcome inhibition to progression of drug-resistant cancer cells.[39, 40] In this study, the cytotoxicity of DOX against

MDA-MB-231 was raised up by using the pH-sensitive MPEG-b-PNLG nanogel as a carrier. The malnourished cell-killing effect of free DOX might be a result of the acquired drug resistance. Conversely, nanogels with pH-sensitive cores can increase the intracellular retention time of DOX or induce a mitochondria-independent apoptotic pathway.[41] As a result, viability was remarkably decreased due to the retained intracellular activities of DOX. These data indicated that the DOX-loaded nanogels are promising for therapeutic applications.

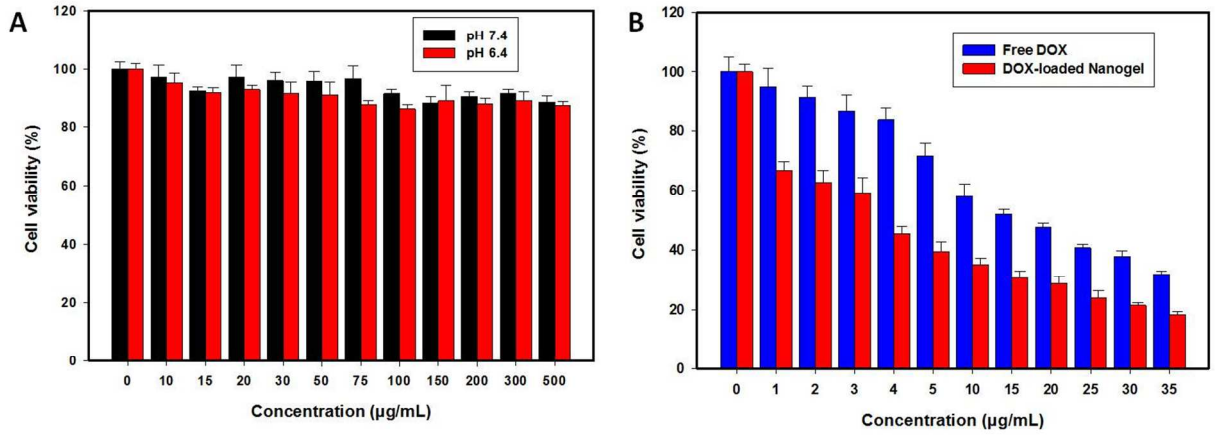

Figure 4. (A) Biocompatibility of MPEG-b-PNLG nanogels on 293T cells at various nanogel concentrations. (B) Cancer cell-killing effect of free DOX and DOX-loaded nanogels.

The internalization of DOX-loaded nanogels was further studied on MDA-MB-231 cells (at a DOX concentration of 3 μg/mL). The intensity of intracellular DOX was measured as a function of treatment time in the FACS assay. The FACS histograms of free DOX and DOX-loaded nanogels at 1 and 3 hr are depicted in **Figure 5**. This figure demonstrated that DOX-loaded nanogels achieved a significant increase in intracellular concentration of the drug than free DOX. The detected fluorescence intensity correlates proportionally with the drug taken up by the cells. Therefore, at the same DOX concentration, the intracellular accumulation of DOX was enhanced

by using MPEG-b-PNLG nanogels as carriers. Confocal laser scanning microscope (CLSM) was utilized to capture the fluorescence images of intracellular DOX. It can be seen from **Figure 6**, the fluorescence intensity of DOX increased in a time-dependent manner. When the same DOX concentration (3 μg/mL) is used, the amount of DOX-loaded nanogels taken up by cells were notably higher than that of free DOX in all investigated time points, which was in consistent with the FACS results. The intracellular release of DOX from nanogels could also be observed in CLSM images (**Figure 6**). After incubation for 1 hr, most DOX-loaded nanogels are in the cytosol; however, with the incubation time increased to 3 hr, DOX was detected to be released to perinuclear and nuclear regions. The appearance of DOX in the nucleus could be attributed to the release of DOX from nanogels after the cleavage of imine bonds in the intracellular acidic environment. The improved intracellular accumulation of DOX-loaded nanogels might enhance the antitumor efficiency of DOX.

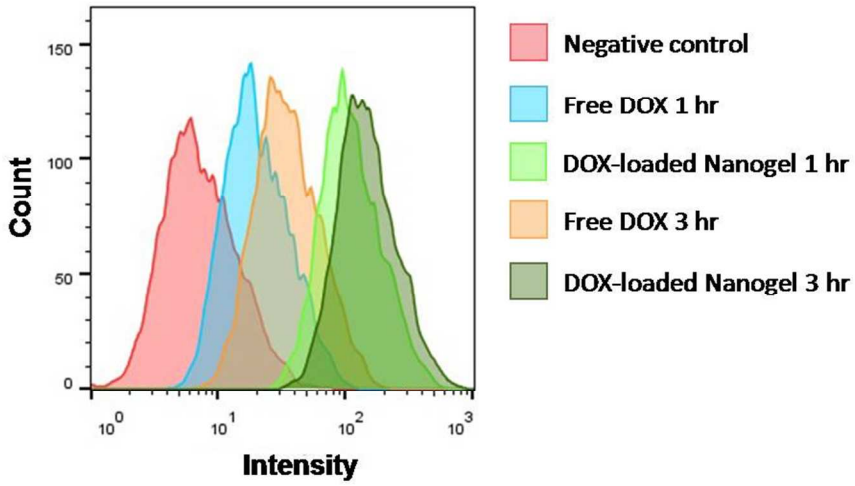

Figure 5. FACS histogram comparison of free DOX and DOX-loaded nanogels with various incubation time (1 hr and 3 hr).

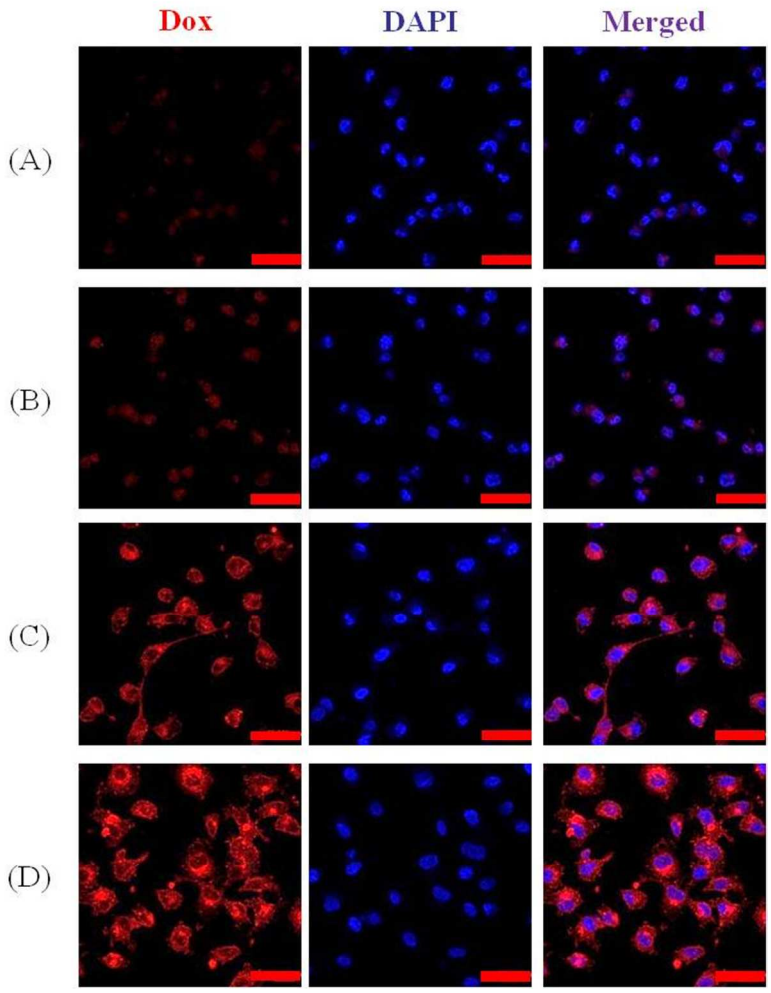

Figure 6. CLSM images of cells incubated with free DOX for (A) 1 hr and (B) 3 hr and cells incubated with DOX-loaded nanogels for (C) 1 hr and (D) 3 hr. (Scale bar: 50 μm)

CONCLUSIONS

In conclusion, a pH-sensitive and polypeptide-based nanogel system was constructed from hydrophilic PNLG. By using hydrophobic TPA as a crosslinker, the obtained nanogels could encapsulate a hydrophobic and small-molecule drug inside its hydrophobic core. This DOX-loaded nanocarrier could rapidly release the encapsulated DOX under acidic conditions such as an intracellular endosome. Furthermore, this system possessed a higher anticancer activity

against MDA-MB-231 cells than free DOX. This pH-sensitive drug delivery system, with its high stability and rapid response, can be suggested as a potential platform for enhanced tumor therapy.

ASSOCIATED CONTENT

Supporting Information

The Supporting Information includes additional Figures S1-S4 and Table S1 showing GPC of the MPEG-b-PNLG polymer; sizes of MPEG-b-PNLG nanogels from different batches; count rates of MPEG-b-PNLG nanogels at different gelling time; size of MPEG-b-PNLG nanogels at different CHO/NH_2 ratios; FT-IR spectrum of MPEG-b-PNLG copolymer, nanogels and nanogels after disassociation; TEM images of MPEG-b-PNLG nanogels and DOX-loaded nanogels. This material is available free of charge via the Internet at http://pubs.acs.org.

AUTHOR INFORMATION

Corresponding Author

* E-mail: dslee@skku.edu (D. S. L.). Tel: +82-31-290-7282

Notes

The authors declare no competing financial interests.

ACKOWNLEDGEMENTS

This research was supported by the Basic Science Research Program through a National Research Foundation of Korea grant funded by the Korean Government (MEST) (NRF-

2017R1A5A1070259) and the National Research Foundation of Korea (NRF) funded by The Ministry of Science, ICT & Future Planning (NRF-2017R1D1A1B03033988).

REFERENCES

(1) Soni, K. S.; Desale, S. S.; Bronich, T. K. Nanogels: An overview of properties, biomedical applications and obstacles to clinical translation. *J. Control. Release* **2016**, *240*, 109-126.

(2) Kabanov, A. V.; Vinogradov, S. V. Nanogels as pharmaceutical carriers: finite networks of infinite capabilities. *Angew. Chem., Int. Ed.* **2009**, *48*, 5418-5429.

(3) Molina, M.; Asadian-Birjand, M.; Balach, J.; Bergueiro, J.; Miceli, E.; Calderon, M. Stimuli-responsive nanogel composites and their application in nanomedicine. *Chem. Soc. Rev.* **2015**, *44*, 6161-6186.

(4) Chen, S.; Bian, Q.; Wang, P.; Zheng, X.; Lv, L.; Dang, Z.; Wang, G. Photo, pH and redox multi-responsive nanogels for drug delivery and fluorescence cell imaging. *Polym. Chem.* **2017**, *8*, 6150-6157.

(5) Luque-Michel, E.; Imbuluzqueta, E.; Sebastián, V.; Blanco-Prieto, M. J. Clinical advances of nanocarrier-based cancer therapy and diagnostics. *Expert Opin. Drug Deliv.* **2017**, *14*, 75-92.

(6) Sampathkumar, K.; Arulkumar, S.; Ramalingam, M. Advances in stimuli responsive nanobiomaterials for cancer therapy. *J. Biomed. Nanotechnol.* **2014**, *10*, 367-382.

(7) Thambi, T.; Park, J. H.; Lee, D. S. Hypoxia-responsive nanocarriers for cancer imaging and therapy: recent approaches and future perspectives. *Chem. Commun.* **2016**, *52*, 8492-8500.

(8) Kobayashi, H.; Watanabe, R.; Choyke, P. L. Improving conventional enhanced permeability and retention (EPR) effects; what is the appropriate target? *Theranostics* **2013**, *4*, 81-89.

(9) Chen, L. Q.; Randtke, E. A.; Jones, K. M.; Moon, B. F.; Howison, C. M.; Pagel, M. D. Evaluations of tumor acidosis within *in vivo* tumor models using parametric maps generated with acidoCEST MRI. *Mol. Imaging Biol.* **2015**, *17*, 488-496.

(10) Justus, C. R.; Sanderlin, E. J.; Yang, L. V. Molecular connections between cancer cell metabolism and the tumor microenvironment. *Int. J. Mol. Sci.* **2015**, *16*, 11055-11086.

(11) Kato, Y.; Ozawa, S.; Miyamoto, C.; Maehata, Y.; Suzuki, A.; Maeda, T.; Baba, Y. Acidic extracellular microenvironment and cancer. *Cancer Cell Int.* **2013**, *13*, 89.

(12) Kanamala, M.; Wilson, W. R.; Yang, M.; Palmer, B. D.; Wu, Z. Mechanisms and biomaterials in pH-responsive tumour targeted drug delivery: A review. *Biomaterials* **2016**, *85*, 152-167.

(13) Gao, G. H.; Li, Y.; Lee, D. S. Environmental pH-sensitive polymeric micelles for cancer diagnosis and targeted therapy. *J. Control. Release* **2013**, *169*, 180-184.

(14) Han, S.-S.; Li, Z.-Y.; Zhu, J.-Y.; Han, K.; Zeng, Z.-Y.; Hong, W.; Li, W.-X.; Jia, H.-Z.; Liu, Y.; Zhuo, R.-X.; Zhang, X.-Z. Dual-pH sensitive charge-reversal polypeptide micelles for tumor-triggered targeting uptake and nuclear drug delivery. *Small* **2015**, *11*, 2543-2554.

(15) Karimi, M.; Eslami, M.; Sahandi-Zangabad, P.; Mirab, F.; Farajisafiloo, N.; Shafaei, Z.; Ghosh, D.; Bozorgomid, M.; Dashkhaneh, F.; Hamblin, M. R. pH-Sensitive stimulus-responsive nanocarriers for targeted delivery of therapeutic agents. *Wiley Interdiscip Rev Nanomed Nanobiotechnol.* **2016**, *8*, 696-716.

(16) Luan, S.; Zhu, Y.; Wu, X.; Wang, Y.; Liang, F.; Song, S. Hyaluronic-acid-based pH-sensitive nanogels for tumor-targeted drug delivery. *ACS Biomater. Sci. Eng.* **2017**, *3*, 2410-2419.

(17) Chacko, R. T.; Ventura, J.; Zhuang, J.; Thayumanavan, S. Polymer nanogels: a versatile nanoscopic drug delivery platform. *Adv. Drug Deliv. Rev.* **2012**, *64*, 836-851.

(18) Pan, Y.-J.; Chen, Y.-Y.; Wang, D.-R.; Wei, C.; Guo, J.; Lu D.-R.; Chu, C.-C.; Wang, C.-C. Redox/pH dual stimuli-responsive biodegradable nanohydrogels with varying responses to dithiothreitol and glutathione for controlled drug release. *Biomaterials* **2012**, *33*, 6570-6579.

(19) Wu, H.; Jin, H.; Wang, C.; Zhang, Z.; Ruan, H.; Sun, L.; Yang, C.; Li, Y.; Qin, W.; Wang, C. Synergistic cisplatin/doxorubicin combination chemotherapy for multidrug-resistant cancer via polymeric nanogels targeting delivery. *ACS Appl. Mater. Interfaces* **2017**, *9*, 9426-9436.

(20) Li, M.; Tang, Z.; Sun, H.; Ding, J.; Song, W.; Chen, X. pH and reduction dual-responsive nanogel cross-linked by quaternization reaction for enhanced cellular internalization and intracellular drug delivery. *Polym. Chem.* **2013**, *4*, 1199-1207.

(21) Yusa, S.; Sugahara, M.; Endo, T.; Morishima, Y. Preparation and characterization of a pH-responsive nanogel based on a photo-cross-linked micelle formed from block copolymers with controlled structure. *Langmuir* **2009**, *25*, 5258-5265.

(22) Daly, W. H.; Poche D. The preparation of N-carboxyanhydrides of α-amino acids using bis (trichloromethyl) carbonate. *Tetrahedron Lett.* **1988**, *29*, 5859-5862.

(23) Choi, J. W.; Kim, J.; Bui, Q. N.; Li, Y.; Yun, C. O.; Lee, D. S.; Kim, S. W. Tuning surface charge and PEGylation of biocompatible polymers for efficient delivery of nucleic acid or adenoviral vector. *Bioconjugate Chem.* **2015**, *26*, 1818-1829.

(24) Kim, J.; Li, Y.; Kim, S. W.; Lee, D. S.; Yun, C. O. Therapeutic efficacy of a systemically delivered oncolytic adenovirus–biodegradable polymer complex. *Biomaterials* **2013**, *34*, 4622-4631.

(25) Yang, H. Y.; Jang, M. S.; Gao, G. H.; Lee, J. H.; Lee, D. S. pH-Responsive biodegradable polymeric micelles with anchors to interface magnetic nanoparticles for MR imaging in detection of cerebral ischemic area. *Nanoscale* **2016**, *8*, 12588-12598.

(26) Li, Y.; Gao, G. H.; Lee, D. S. pH-sensitive polymeric micelles based on amphiphilic polypeptide as smart drug carriers. *J. Polym. Sci., Part A: Polym. Chem.* **2013**, *51*, 4175-4182.

(27) Bui, Q. N.; Li, Y.; Jang, M.-S.; Huynh, D. P.; Lee, J. H.; Lee, D. S. Redox-and pH-sensitive polymeric micelles based on poly (β-amino ester)-grafted disulfide methylene oxide poly (ethylene glycol) for anticancer drug delivery. *Macromolecules* **2015**, *48*, 4046-4054.

(28) Thambi, T.; Saravanakumar, G.; Chu, J.-U.; Heo, R.; Ko, H.; Deepagan, V. G.; Kim, J.-H.; Park, J. H. Synthesis and physicochemical characterization of reduction-sensitive block copolymer for intracellular delivery of doxorubicin. *Macromol. Res.* **2013**, *21*, 100-107.

(29) Yoo, H. S.; Lee, E. A.; Park, T. G. Doxorubicin-conjugated biodegradable polymeric micelles having acid-cleavable linkages. *J. Control. Release* **2002**, *82*, 17-27.

(30) Peruzzo, M.; Milani, G. P.; Garzoni, L.; Longoni, L.; Simonetti, G. D.; Bettinelli, A.; Fossali, E. F.; Bianchetti, M. G. Body fluids and salt metabolism-Part II. *Ital. J. Pediatr.* **2010**, *36*, 78.

(31) Bianchetti, M. G.; Simonetti, G. D.; Bettinelli, A. Body fluids and salt metabolism-Part I. *Ital. J. Pediatr.* **2009**, *35*, 36.

(32) Kataoka, K.; Harada, A.; Nagasaki, Y. Block copolymer micelles for drug delivery: design, characterization and biological significance. *Adv. Drug Deliv. Rev.* **2001**, *47*, 113-131.

(33) Chang, L.; Deng, L.; Wang, W.; Lv, Z.; Hu, F.; Dong, A.; Zhang, J. Poly(ethylene glycol)-b-poly(ε-caprolactone-co-γ-hydroxyl-ε-caprolactone) bearing pendant hydroxyl groups as nanocarriers for doxorubicin delivery. *Biomacromolecules* **2012**, *13*, 3301-3310.

(34) Holohan, C.; Van Schaeybroeck, S.; Longley, D. B.; Johnston, P. G. Cancer drug resistance: an evolving paradigm. *Nat. Rev. Cancer* **2013**, *13*, 714-726.

(35) Al-Ghamdi, S. S. Time and dose dependent study of doxorubicin induced DU-145 cytotoxicity. *Drug Metab. Lett.* **2008**, *2*, 47-50.

(36) Lupertz, R.; Watjen, W.; Kahl, R.; Chovolou, Y. Dose-and time-dependent effects of doxorubicin on cytotoxicity, cell cycle and apoptotic cell death in human colon cancer cells. *Toxicology* **2010**, *271*, 115-121.

(37) Aroui, S.; Brahim, S.; Hamelin, J.; De Waard, M.; Breard, J.; Kenani, A. Conjugation of doxorubicin to cell penetrating peptides sensitizes human breast MDA-MB 231 cancer cells to endogenous TRAIL-induced apoptosis. *Apoptosis* **2009**, *14*, 1352-1365.

(38) Aroui, S.; Brahim, S.; De Waard, M.; Breard, J.; Kenani, A. Efficient induction of apoptosis by doxorubicin coupled to cell-penetrating peptides compared to unconjugated doxorubicin in the human breast cancer cell line MDA-MB 231. *Cancer Lett.* **2009**, *285*, 28-38.

(39) Ogawara, K.; Un, K.; Tanaka, K.; Higaki, K.; Kimura, T. *In vivo* anti-tumor effect of PEG liposomal doxorubicin (DOX) in DOX-resistant tumor-bearing mice: Involvement of cytotoxic effect on vascular endothelial cells. *J. Control. Release* **2009**, *133*, 4-10.

(40) Deng, X.; Cao, M.; Zhang, J.; Hu, K.; Yin, Z.; Zhou, Z.; Xiao, X.; Yang, Y.; Sheng, W.; Wu, Y.; Zeng, Y. Hyaluronic acid-chitosan nanoparticles for co-delivery of MiR-34a and doxorubicin in therapy against triple negative breast cancer. *Biomaterials* **2014**, *35*, 4333-4344.

(41) Yi, X.-Q.; Zhang, Q.; Zhao, D.; Xu, J.-Q.; Zhong, Z.-L.; Zhuo, R.-X.; Li, F. Preparation of pH and redox dual-sensitive core crosslinked micelles for overcoming drug resistance of DOX. *Polym. Chem.* **2016**, *7*, 1719-1729.

Table of Contents:

Title: One-Step Preparation of pH-Responsive Polymeric Nanogels as An Intelligent Drug Delivery System for Tumor Therapy

Authors: Yi Li, Quang Nam Bui, Le Thai Minh Duy, Hong Yu Yang and Doo Sung Lee

Graph: